



# A new damage model accounting the effect of joint orientation for the jointed rock mass

Changtai Zhou<sup>1</sup> · Murat Karakus<sup>1</sup> · Chaoshui Xu<sup>1,2</sup> · Jiayi Shen<sup>3</sup>

Received: 1 August 2019 / Accepted: 3 March 2020 / Published online: 25 March 2020  
© Saudi Society for Geosciences 2020

## Abstract

Damage accumulation in the rock mass leading to failure is influenced by the properties of pre-existing discontinuities. In order to simulate rock mass behaviour realistically, many damage models have been proposed. Amongst them, limited damage models consider joint orientation, one of the significant properties of discontinuities impacting the rock mass failure, in the strongly anisotropic rock masses. In this study, we propose a statistical damage model using the Weibull distribution which takes into account joint orientation by incorporating the Jaeger's and modified Hoek-Brown failure criteria for jointed rock masses. The proposed statistical damage model is validated using experimental results. Furthermore, verification of the proposed model is conducted by distinct element method using Particle Flow Code (PFC). To investigate the influence of the shape parameter ( $m$ ) and scale parameter ( $F_0$ ) of the Weibull distribution on the statistical damage model predictions, a sensitivity analysis is carried out. It is found that the parameter  $m$  only depends on strain parameter  $k$ . On the other hand, the parameter  $F_0$  is indirectly related to the failure strength of the jointed rock mass in the proposed damage model. Considerable influence of joint stiffness on the damage variable  $D$ , damage evolution rate  $D_r$  and rock mass responses are also identified.

**Keywords** Damage model · Joint orientation · Jointed rock mass · Bonded particle model

## Abbreviations

$P(F)$	The percentage of damaged elements out of the total number of microscopic elements.	$N$	The total number of all microscopic elements
$F$	The element strength parameter depending on the strength criterion used	$n$	The number of all failed microscopic elements under a certain loading
$F_0$	Scale parameter of the Weibull distribution	$\sigma_i$ (MPa)	The nominal stress, $i = 1, 3$
$m$	Shape parameter or a homogeneous index of Weibull distribution	$\sigma_i^*$ (MPa)	The effective stress, $i = 1, 3$
$D$	Damage variable	$\nu$	Poisson's ratio of the material
		$\varepsilon_1$	The strain on the principal principal stress direction
		$\sigma_{1f}$ (MPa)	Peak stress at failure
		$\varepsilon_{1f}$	Peak strain at failure
		$c$ (MPa)	Cohesion
		$\phi$ (°)	Internal friction angle
		$c_j$ (MPa)	Joint cohesion
		$\phi_j$ (°)	Joint friction angle
		$\beta$ (°)	Joint orientation
		$m_i$	A material constant of Hoek-Brown
		$k_0$	A constant value related to the cohesion and internal friction angle of the rock
		$k_\beta$	Anisotropy parameter
		$E$ (GPa)	Young's modulus of rock
		$E_\beta$ (GPa)	Deformation modulus of the jointed rock mass

Responsible Editor: Zeynal Abiddin Erguler

✉ Murat Karakus  
murat.karakus@adelaide.edu.au

<sup>1</sup> School of Civil, Environmental and Mining Engineering, The University of Adelaide, Adelaide, Australia

<sup>2</sup> School of Resource and Environmental Engineering, Wuhan University of Science and Technology, Wuhan, China

<sup>3</sup> Institute of Port, Coastal and Offshore Engineering, Zhejiang University, Hangzhou, China

$\delta$ (m)	A mean vertical spacing interval in rock that contains a single set of horizontal joints
$k_n$ (GPa)	Joint normal stiffness
$k_s$ (GPa)	Joint shear stiffness
$k$	Strain parameter
COV (%)	Coefficient of variation

## Introduction

The deformation behaviour of rock material is a fundamental topic in rock engineering (Li et al. 2012; Peng et al. 2015). Accurate estimation of rock strength and deformation properties is critical for the stability analysis of rock engineering applications such as rock slopes, rock tunnels and underground excavations. In nature, the rock mass consists of intact rock and discontinuities such as bedding planes, joints and cleavages. The strength and the mechanical properties of the rock mass are controlled by the mechanical and geometrical properties of the discontinuities and intact rocks (Guo et al. 2017; Jin et al. 2016; Tiwari and Rao 2006; Wasantha et al. 2015; Yang et al. 1998; Zhou et al. 2014). In this study, the rock mass is defined as the intact rock separated by the joints, bedding planes, folds etc. at the lab- or in-situ-scale. Therefore, the deformation behaviours of the rock mass can be largely influenced by the geometrical and mechanical properties of joints, especially for anisotropic rock mass.

Many experimental investigations (Chen et al. 2016; Donath 1961; Hoek 1964; Jiang et al. 2014; Jin et al. 2016; McIlmore and Gray 1967; Prudencio and Van Sint Jan 2007; Ramamurthy et al. 1988; Yang et al. 1998) published characterized deformation properties and failure mechanisms in anisotropic rock masses. The results from these studies indicate that the failure strength and deformation are closely associated with joint orientation or bedding orientation (see Fig. 1). The corresponding joint orientation is also demonstrated in Fig. 1. The failure strength reaches its maximum value at  $\beta = 90^\circ$ , while its minimum value located around  $\beta = 60^\circ$ . Three failure modes are observed in the experimental results (Tien and Tsao 2000): sliding mode along the discontinuity or joint, shearing mode along the intact rock and mixed-mode. These laboratory results lay the foundation for failure analysis of anisotropic rock masses.

To describe the stress-strain relationship for rock materials, the statistical damage model (SDM) has been widely employed for different applications based on the statistical theory and continuum damage mechanics. The SDM was first proposed by Krajcinovic and Silva (1982) to reflect the process of micro-crack initiation, propagation, and coalescence and was employed to explore the damage process of concretes. Later, the concept of SDM was adopted and extended to grasp the complicated behaviours of rocks (Cao et al. 2018; Cao et al. 2010; Deng and Gu 2011; Li et al. 2012; Liu

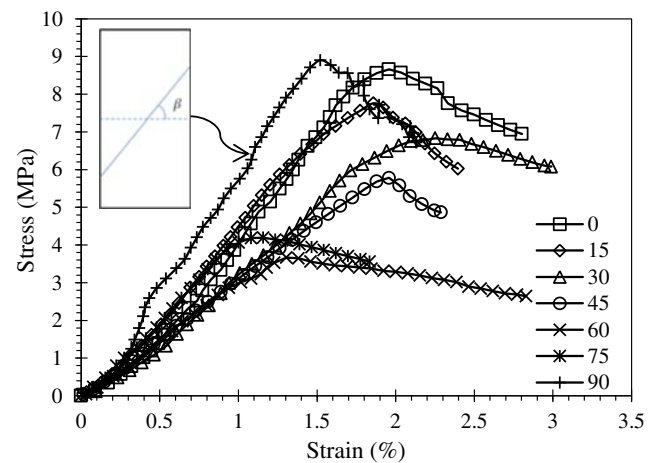


**Fig. 1** Behaviour of rock-like materials with different joint orientation (after Jin et al. 2016)

and Yuan 2015; Tang et al. 1998). The initial damage (crack closure stage) was identified and modelled by introducing initial voids (Cao et al. 2018) and dissipated energy corresponding to the initial damage (Yang et al. 2015). The residual strength of rocks induced by the confining pressure was further considered by different researchers. For example, a coefficient  $C_n$  was introduced by Wang et al. (2007) to improve the description of residual strength. Zhao et al. (2016) adopted the damage tolerance principle to reflect the residual strength of the rocks. The impact on the mechanical properties of rocks was captured by the SDM using the coefficient of viscosity (Li et al. 2015) and over-stress model (Zhao et al. 2014).

To address the anisotropic characteristics of the jointed rock mass, which may be vital to the stability of slopes and caverns (Hudson and Harrison 2000; Jia et al. 2012; Kostić 2017), the damage tensors were employed in SDM in most cases. Kawamoto et al. (1988) and Swoboda et al. (1998) adopted a second-order damage tensor to reflect rock mass anisotropy due to pre-existing joints. In their damage models, geometrical parameters of joints such as orientation, length and density were used to describe the anisotropic characteristics of the jointed rock mass. Recently, based on these works, Yang et al. (2019) employed the normal vector and area of joints to describe the joints based on damage mechanics. However, in strongly anisotropic materials, these models do not correctly describe the failure modes: shear failure in the intact rock matrix and sliding failure along the joint and thus they may underestimate the strength of the rock mass (Liu and Yuan 2015). Therefore, it is still necessary to develop a new damage model for the jointed rock mass considering the joint orientation and failure modes.

In this paper, inspired by the previous studies mentioned above, a new statistical damage model for a rock mass considering joint orientation is derived based on the Weibull distribution. Fundamentals of the statistical damage model and its derivation are explained in “Statistical damage model”

section. Validation and verification of the proposed damage model are presented in “Validation and verification of the proposed damage model” section. Particle Flow Code used for verification is explained in “Validation and verification of the proposed damage model” section. Finally, a sensitivity analysis for the damage distribution parameters and rock mass response is carried out in “Sensitivity analysis of damage distribution parameters and the damage variables and rock mass response” section.

## Statistical damage model

### Damage model development

Conceptually, a rock is composed of a large number of microscopic elements. When the rock is subjected to external loading, microscopic elements will fail, and defects or micro-cracks are created, which then coalesce to form macro-cracks. This is basically the damage accumulation process taking place in the rock as a response to an external load. Statistically, the strength of these microscopic elements can follow a certain type of distribution with the most commonly suggested ones as power function distribution and Weibull distribution. Therefore, a statistical approach may better describe the mechanical behaviour of rocks at the micro-level (Deng and Gu 2011).

The Weibull distribution used to describe the distribution of the strength of microscopic elements in the damage model can be written as:

$$P(F) = \frac{m}{F_0} \left(\frac{F}{F_0}\right)^{m-1} \exp\left[-\left(\frac{F}{F_0}\right)^m\right] \tag{1}$$

where  $F$  is the element strength parameter depending on the failure criterion used, which can be regarded as stress level when strength criterion (Zhou et al. 2017) is used or strain when maximum strain criterion (Liu and Yuan 2015) is adopted;  $m$  is the shape parameter or a homogeneous index of Weibull distribution;  $F_0$  is the scale parameter of the Weibull distribution.

Assuming  $N$  is the number of all microscopic elements within the rock and  $n$  denotes the number of failed microscopic elements under a certain external load, the damage variable  $D$  (between 0 and 1) can be directly defined as (Tang and Kaiser 1998):

$$D = \frac{n}{N} \tag{2}$$

If all microscopic elements are subjected to the same local stress of  $F$ , the total failed microscopic elements  $n$  can be calculated as:

$$n = N \int_0^F P(F) dF = N \left\{ 1 - \exp\left[-\left(\frac{F}{F_0}\right)^m\right] \right\} \tag{3}$$

i.e., the damage variable  $D$  can be expressed as:

$$D = 1 - \exp\left[-\left(\frac{F}{F_0}\right)^m\right] \tag{4}$$

Under biaxial compression, two effective stresses ( $\sigma_1, \sigma_3$ ) of the rock mass can be expressed using nominal stresses ( $\sigma_1, \sigma_3$ ):

$$\sigma_i^* = \sigma_i / (1 - D) \tag{5}$$

with  $i = 1, 3$ .

According to the generalized Hooke’s law and the damage, the strain can be expressed as:

$$\varepsilon_1 = \frac{1}{E} (\sigma_1^{*-\nu} \sigma_3^*) = \frac{1}{E(1-D)} (\sigma_1 - \nu \sigma_3) \tag{6}$$

where  $\nu$  is the Poisson’s ratio of the material. Substituting Eq. (4) into Eq. (6), the stress-strain relationship is obtained on the major principal stress direction:

$$\sigma_1 = E \varepsilon_1 \exp\left[-\left(\frac{F}{F_0}\right)^m\right] + \nu \sigma_3 \tag{7}$$

As an example to demonstrate this model, the damage variable  $D$ ,  $E = 50$  GPa,  $\sigma_3 = 0$  MPa and  $F_0 = 0.01$  with maximum strain criterion were adopted here and the results are plotted in Fig. 2 for different  $m$  values. As can be seen, a higher value of  $m$  corresponds to narrower distribution of the element strengths, hence greater variation in damage variable  $D$  against strain and a sharper decrease of the stress after the peak load. In other words, when  $m$  value is increased, the rock behaves in a more brittle fashion, and its strength increases accordingly.

Next, the strength of the microscopic elements must be determined. As shown in Fig. 2, the maximum strain criterion can be used to describe the microscopic element strength. However, it could not reflect the influence of complicated stress state of the microscopic element. Therefore, many studies (Deng and Gu 2011; Li et al. 2012; Xu and Karakus 2018) tried to consider the rock failure criterion for a microscopic element in stress space and proposed new expressions for the microscopic element. In general, the failure criterion of the microscopic element can be expressed in the following form:

$$f(\sigma^*) - k_0 = 0 \tag{8}$$

where  $k_0$  is a constant value related to the cohesion and internal friction angle of the rock.  $F = f(\sigma^*) = f(\sigma)/(1 - D)$  reflects the strength of microscopic element, depending on the failure criteria adopted in the damage model.

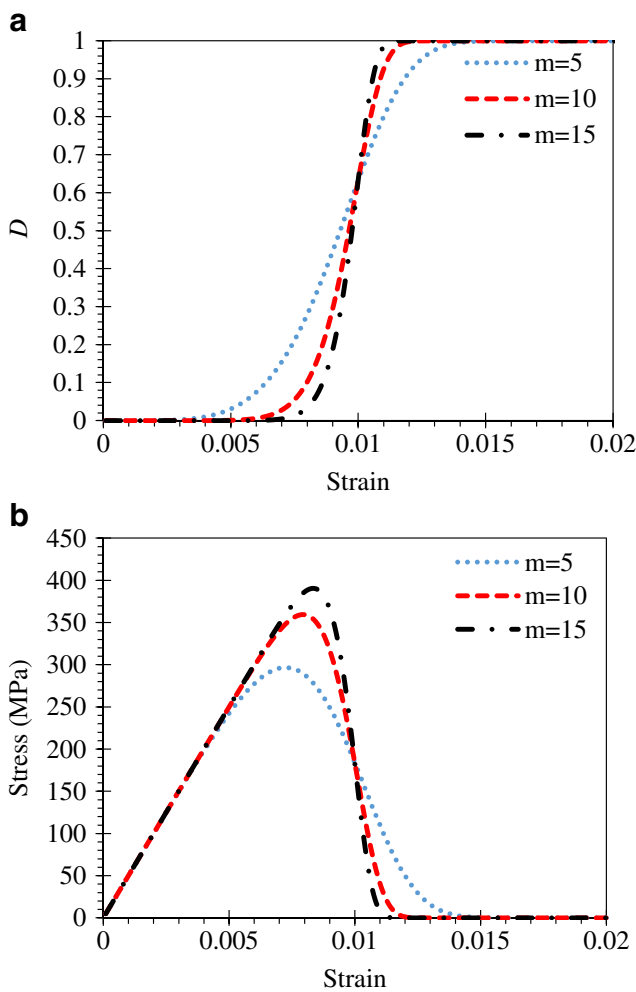


**Fig. 2** Microscopic damage variable and the strength of intact rock. **a** Damage variable vs. strain. **b** Corresponding stress-strain response

Rearranging Eq. (6), one can obtain:

$$1-D = \frac{(\sigma_1 - \nu\sigma_3)}{E\varepsilon_1} \tag{9}$$

Then substituting in Eq. 8, the following equation can be obtained:

$$F = \frac{f(\sigma)}{\sigma_1 - \nu\sigma_3} E\varepsilon_1 \tag{10}$$

To derive the rock mass response and calculate damage variable  $D$ , the damage parameters  $m$  and  $F_0$  should be determined. In this process, the ‘Extremum method’ was used in previous studies (Cao et al. 2010; Deng and Gu 2011), where the peak point of the measured stress-strain curve can be used. At the peak point, the derivative of  $\sigma_1$  with corresponding  $\varepsilon_1$  should be zero, i.e.:

$$\varepsilon_1 = \varepsilon_{1f}, \sigma_1 = \sigma_{1f} \tag{11}$$

$$\frac{d\sigma_1}{d\varepsilon_1} = 0 \tag{12}$$

where  $\sigma_{1f}$  and  $\varepsilon_{1f}$  are stress and strain corresponding to the peak point. Based on the Eq. (12), one can obtain:

$$m\varepsilon_1 \left(\frac{F}{F_0}\right)^{m-1} \frac{1}{F_0} \frac{dF}{d\varepsilon_1} = 1 \tag{13}$$

From Eq. (9), one can easily obtain the following equation:

$$\frac{dF}{d\varepsilon_1} = \frac{f(\sigma)}{\sigma_1 - \nu\sigma_3} E = \frac{F}{\varepsilon_1} \tag{14}$$

Then the distribution parameter  $m$  and  $F_0$  can be calculated by substituting Eqs. (13) and (11) into Eq. (7):

$$m = \frac{1}{\ln(E\varepsilon_{1f}/(\sigma_{1f} - \nu\sigma_3))} \tag{15}$$

$$F_0 = \sqrt[m]{m} F_f, \varepsilon_1 = \varepsilon_{1f} \tag{16}$$

### Implementation of failure criteria into the proposed damage model

Appropriate failure criterion should be determined for the microscopic elements in the damage model (Xu and Karakus 2018). Due to the pre-existing joint, the commonly used failure criteria should be modified to account for the influence of joint orientation. In nature, the anisotropic rock masses demonstrated the anisotropic characteristics due to various forms of weakness and generally can be divided into two groups: the rock masses with a strong discontinuity or a set of parallel joints and the inherently anisotropic rock masses. Therefore, two failure criteria including Jaeger’s criterion and Hoek-Brown criterion are integrated into the proposed damage model.

#### Jaeger’s failure criterion

We used Jaeger’s failure criterion to derive the damage parameters for the Weibull damage model:

$$\sigma_1 = \begin{cases} \frac{1 + \sin\phi}{1 - \sin\phi} \sigma_3 + \frac{2c \cos\phi}{1 - \sin\phi}, & \beta < \phi_j \text{ or } \beta = 90^\circ \\ \sigma_3 + \frac{2c_j + 2\sigma_3 \tan\phi_j}{\sin 2\beta (1 - \tan\phi_j \tan\beta)}, & \phi_j \leq \beta < 90^\circ \end{cases} \tag{17}$$

where  $c$  and  $\phi$  are cohesion and internal friction angle of the rock;  $c_j$  and  $\phi_j$  are joint cohesion and friction angle, respectively, and  $\beta$  is the joint orientation (the angle of the joint from the plane perpendicular to the loading direction). Then the strength of microscopic element in stress space can be expressed in the following equation:

$$\begin{cases} F_1 = \frac{\sigma_1 - \frac{1 + \sin\phi}{1 - \sin\phi} \sigma_3}{\sigma_1 - \nu\sigma_3} E\varepsilon_1, & \beta < \phi_j \text{ or } \beta = 90^\circ \\ F_2 = \frac{\sigma_1 - \left[1 + \frac{2 \tan\phi_j}{\sin 2\beta (1 - \tan\phi_j \tan\beta)}\right] \sigma_3}{\sigma_1 - \nu\sigma_3} E\varepsilon_1, & \phi_j \leq \beta < 90^\circ \end{cases} \quad (18)$$

We can derive the stress-strain relationship by substituting Eq. (18) into Eq. (7):

$$\sigma_1 = \begin{cases} E\varepsilon_1 \exp\left[-\left(\frac{F_1}{F_0}\right)^m\right] + \nu\sigma_3, & \beta < \phi_j \text{ or } \beta = 90^\circ \\ E\varepsilon_1 \exp\left[-\left(\frac{F_2}{F_0}\right)^m\right] + \nu\sigma_3, & \phi_j \leq \beta < 90^\circ \end{cases} \quad (19)$$

where  $F_1$  and  $F_2$  are the expression of microscopic strength derived in Eq. (18).

**Modified Hoek-Brown criterion**

Here, the modified Hoek-Brown model proposed by Saroglou and Tsiambaos (Saroglou and Tsiambaos 2008) incorporating the anisotropic parameter  $k_\beta$  of rock mas is used:

$$\sigma_1 = \sigma_3 + \sigma_c \left(k_\beta m_i \frac{\sigma_3}{\sigma_c} + 1\right)^{0.5} \quad (20)$$

where  $m_i$  is a Hoek-Brown constant, depending on the rock type (texture and mineralogy) (Shen and Karakus 2014),  $\sigma_c$  is the uniaxial compressive strength of the intact rock. Then failure strength of microscopic element using the Hoek-Brown criterion can be expressed in the following equation:

$$F = \frac{\sqrt{(\sigma_1 - \sigma_3)^2 - k_\beta m_i \sigma_c \sigma_3}}{\sigma_1 - \nu\sigma_3} E\varepsilon_1 \quad (21)$$

Accordingly, the stress-strain relationship can be expressed as:

$$\sigma_1 = E\varepsilon_1 \exp\left[-\left(\frac{\sqrt{(\sigma_1 - \sigma_3)^2 - k_\beta m_i \sigma_c \sigma_3}}{\sigma_1 - \nu\sigma_3} E\varepsilon_1}{F_0}\right)^m\right] + \nu\sigma_3 \quad (22)$$

**Damage model implementation**

In order to implement the proposed damage model for further analysis, the basic material parameters such as

cohesion ( $c$ ), internal friction angle ( $\phi$ ), joint cohesion ( $c_j$ ), joint friction angle ( $\phi_j$ ) and joint orientation ( $\beta$ ) should be identified first. Then the failure stress  $\sigma_{1f}$ , deformation modulus  $E_\beta$  and failure strain  $\varepsilon_{1f}$  should be determined to derive the damage distribution parameters  $m$  and  $F_0$ . We can estimate the failure stress  $\sigma_{1f}$  from Eqs. (17) and (20). However, the deformation modulus  $E_\beta$  of the jointed rock mass is influenced by the joint orientation, which can be estimated through the following equation (Gao et al. 2016):

$$\frac{1}{E_\beta} = \frac{1}{E} + \cos^2\beta \left(\frac{\cos^2\beta}{\delta k_n} + \frac{\sin^2\beta}{\delta k_s}\right) \quad (23)$$

where  $\delta$  is a mean vertical spacing interval in rock that contains a single set of joints;  $k_n$  and  $k_s$  are the normal stiffness and shear stiffness on the weak planes, respectively. On the other hand, the failure strain  $\varepsilon_{1f}$  is related to the failure stress  $\sigma_{1f}$  and the deformation modulus  $E_\beta$ :

$$\varepsilon_{1f} \propto \frac{\sigma_{1f}}{E_\beta} \quad (24)$$

Due to the existing crack closure and unstable crack growth stages, the failure strain is larger than  $\frac{\sigma_{1f}}{E_\beta}$ . Therefore, to better estimate the failure strain, a strain parameter  $k$  is introduced here, and the failure strain can be estimated using the following equation:

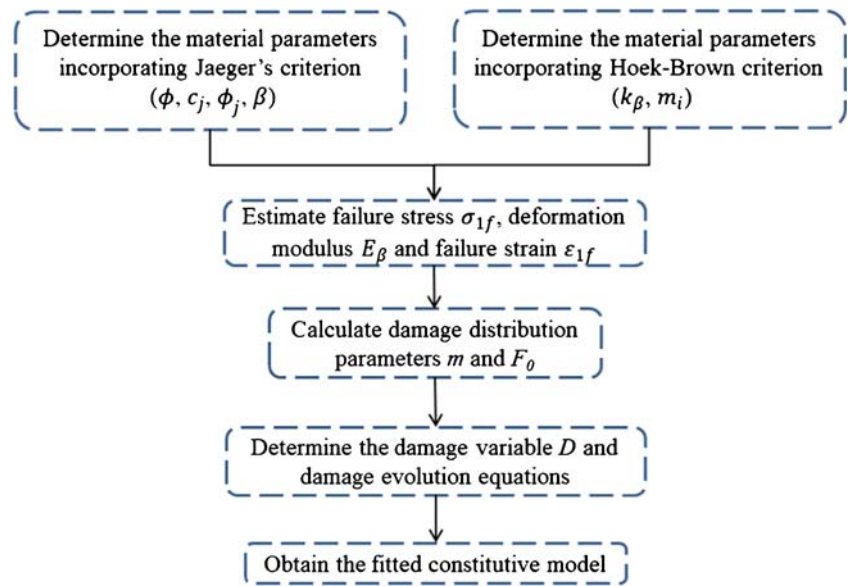
$$\varepsilon_{1f} = (1 + k) \frac{\sigma_{1f}}{E_\beta} \quad (25)$$

where  $k$  depends on the plastic strain of the material, which will be discussed in “Sensitivity analysis of damage distribution parameters and the damage variables and rock mass response” section.

The implementation procedure for the proposed damage model is summarized as follows, see Fig. 3:

- (1) Obtain the basic material parameters: rock cohesion  $c$ , internal friction angle  $\phi$ , joint cohesion  $c_j$ , joint friction angle  $\phi_j$  and joint orientation  $\beta$  for the damage model incorporating Jaeger’s criterion; anisotropic parameter  $k_\beta$  and Hoek-Brown constant  $m_i$  for the damage model incorporating the modified Hoek-Brown criterion;
- (2) Estimate failure stress  $\sigma_{1f}$ , deformation modulus  $E_\beta$  and failure strain  $\varepsilon_{1f}$  through Eqs. (17) or (20), (23) and (25), respectively;
- (3) Obtain damage distribution parameters  $m$  and  $F_0$  through Eqs. (15) and (16);
- (4) Substitute damage distribution parameters  $m$  and  $F_0$  into Eq. (19) or (22) to obtain the stress-strain response.

**Fig. 3** Flow chart for damage model implementation



### Validation and verification of the proposed damage model

#### Validation of the proposed damage model

To validate the proposed damage model, the damage model is applied to a group of published experimental data on jointed basalt (Jin et al. 2016) using modified Hoek-Brown criterion. In the experimental test, rock-like material, a mixture of water, river sand and gypsum, was prepared to model the columnar jointed basalt. The joint orientation varies while the joint roughness is kept smooth in the experimental study. The results of the damage model, obtained from Eq. (7), with different joint orientation is presented in Fig. 4, and the corresponding experimental results are also shown for comparison purpose. One can see that the proposed model is capable of describing the main deformation and strength properties of the jointed rock mass, especially the pre-peak region. However, the rock mass responses from the proposed damage model cannot capture the rock compaction characteristics in the initial stage of rock mass response when joint orientation <math>< 30^\circ</math>. The rock compaction in the initial stage of rock mass response relates to the crack closure when joint orientation <math>< 30^\circ</math>. The damage variable  $D$  may be modified in future study to capture this phenomenon.

#### Verification of the proposed damage model by PFC

The proposed damage model is verified by comparison of the stress-strain response of a rock mass from the proposed model and results are obtained from the bonded particle model, PFC in this study. The synthetic rock mass (SRM) model consists

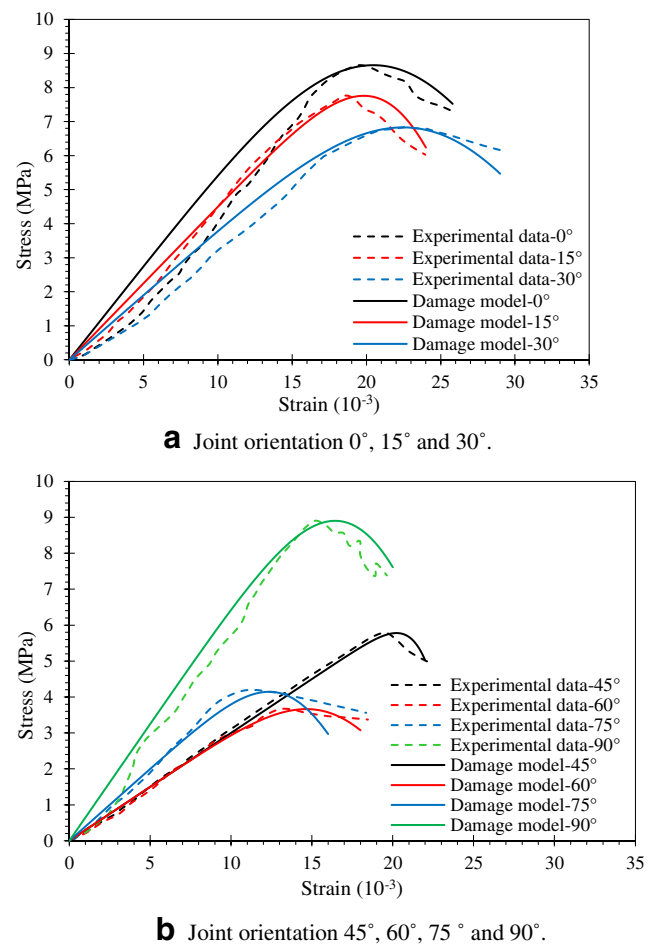


**Fig. 4** Comparison of the proposed damage model and experimental results (Jin et al. 2016) for the jointed rock mass with various joint orientations. **a** Joint orientation 0°, 15° and 30°. **b** Joint orientation 45°, 60°, 75° and 90°

of two components to represent intact rock and discontinuities (Mas Ivars et al. 2011). Intact rock can be represented by bonded particle model (BPM) (Potyondy and Cundall 2004) material which is non-uniform circles or particles assembly connected through contacts. For the current study, the flat joint model (FJM) is employed to simulate a more realistic intact rock, especially for brittle rocks (Vallejos et al. 2016; Zhou et al. 2019, 2018). On the other hand, the smooth joint model (SJM) is implemented into the flat joint contacts to represent joint in PFC.

### Intact rock representation

In this study, the Hawkesbury sandstone was chosen for the verification study. A rectangular numerical model of 54 mm × 108 mm containing random non-uniform particles assembly was subjected to uniaxial compression tests to obtain macro-properties for calibration. The loading rate is set to small enough (0.02 m/s) to ensure the quasi-static loading condition (Zhang and Wong 2014, 2013).

The PFC parameters calibrated using experimental data reported by Wasantha et al. (2013), and are given in Table 1. A good agreement between experimental and PFC model results was achieved, where the coefficient of variation (COV) was found to be less 1%. The calibrated micro-parameters for Hawkesbury sandstone are summarized in Table 2. Figure 5 shows the intact rock response of UCS tests conducted in PFC.

### Joint representation

To simulate the behaviour of the joint within a rock mass, the smooth joint contact model was proposed by Pierce et al. (2007) and explored in detail by Mas Ivars et al. (2008). The smooth joint model provides the behaviour of a planar interface with dilation regardless of the local particle contact orientations along with the interface. The two particles using a smooth joint contact model may slide past each other instead of moving around each other of FJM.

Generally, these macro-properties include normal stiffness, shear stiffness, cohesion and friction angle, and are governed by smooth joint micro-parameters such as bond normal stiffness, bond shear stiffness, bond cohesion and friction angle at the particle level. Bahaaddini et al. (2013) proposed a two-stage calibration procedure: normal deformability test for normal stiffness calibration and direct shear test for the shear

stiffness and coefficient of friction calibration, and using the ISRM suggested method (Ulusay 2014) (see Fig. 6).

In this study, normal stiffness and shear stiffness are set large to minimise their effect on mechanical properties, and the only direct shear test was carried out to match the cohesion and friction angle of Hawkesbury sandstone, which is 2.2 MPa and 32°. The corresponding calibrated cohesion and joint friction angle are 2.19 MPa and 31.79°, respectively. And the calibrated micro-parameters for the smooth-joint model are summarized in Table 3.

### Simulation of a single-jointed rock mass by PFC

In order to verify the proposed damage model, the PFC models with different joint orientations using 0°, 40°, 50°, 60° and 90° are subjected to the uniaxial compression tests. The correctness and robustness of the numerical model were confirmed in our previous study (Zhou et al. 2019). The comparison of the proposed Weibull damage model and the results from the PFC analysis are shown in Fig. 7.

The failure stress of rock mass model when joint orientation  $\beta = 0^\circ$  drops to 46.88 MPa, which is consistent with the experimental results (Wasantha et al. 2013) when one persistent joint exists in the intact specimen. The comparison shows that the proposed damage model is in good agreement with the PFC results at both the pre-peak and post-peak regions. As can be seen from Fig. 7, the proposed damage model can capture the stress-strain response better at pre-peak region than the post-peak region.

### Sensitivity analysis of damage distribution parameters and the damage variables and rock mass response

The damage variables in the proposed damage model are largely influenced by the joint orientation based on the analysis presented in “Statistical damage model” section. Taking the stress-strain in the direction of the major principal strain as an example, we considered  $E = 11.00$  GPa,  $\sigma_{(90)} = 46.88$  MPa,  $\sigma_3 = 0.00$  MPa,  $\nu = 0.20$ ,  $k = 0.2$ ,  $c_j = 6.00$  MPa and  $\phi_j = 0^\circ$  as the reference parameters for sensitivity analysis.

**Table 1** Mechanical properties of Hawkesbury sandstone (Wasantha et al. 2013) and calibrated BPM material

Macro-properties	UCS, MPa	Tensile strength, MPa	Young's modulus, GPa	Poisson's ratio
Experimental results	50.80	4.00	11.00	0.20
PFC results	50.17	4.08	11.02	0.21
COV (%)	0.51	1.40	0.13	0.70

**Table 2** Basic calibrated micro-parameters for Hawkesbury sandstone (Zhou et al. 2018)

PFC model parameters	Micro properties of PFC2D	Description	Value
Microstructure parameters	$w/d$	Ratio of specimen width to the average ball diameter	60
	$r_{max}/r_{min}$	Ratio of maximum to minimum ball radius	1.66
	$g/r_{min}$	Installation-gap ratio	4e-2
	$n_p$	Porosity	0.16
	$N_r$	Number of elements	3
FJM Constitutive parameters	$E^*$ (GPa)	Bond modulus	11.40
	$k^*$	Stiffness ratio	2.5
	$\mu$	Friction coefficient	0.77
	$t_b$ (MPa)	Bond tensile strength	7.10
	$c_b$ (MPa)	Bond cohesion	28.20
	$\Phi_b$ (degree)	Bond friction angle	25

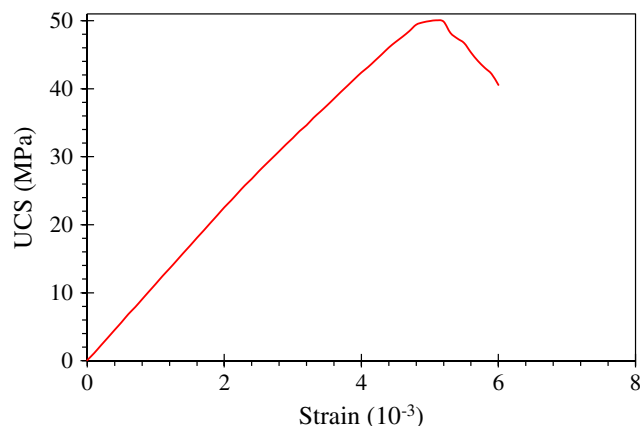
## Damage distribution parameters

### Damage distribution parameter $m$

As mentioned in “Statistical damage model” section, the damage distribution parameter  $m$  is an indicator of material brittleness: more brittle as the damage distribution parameter  $m$  becomes larger. Substituting Eq. (25) into Eq. (15), we can see that the damage distribution parameter only depends on parameter  $k$ :

$$m = \frac{1}{\ln(1+k)} \quad (26)$$

The result (see Fig. 8), shows that damage distribution parameter  $m$  is nonlinear and indirectly proportional to the strain parameter  $k$  for the jointed rock mass. As the parameter  $k$  is directly proportional to the increase of the failure strain, we confirm that the material becomes more brittle as the failure strain becomes smaller. The parameter  $k$  should be

**Fig. 5** Intact rock behaviour under uniaxial compression in PFC

carefully chosen according to the material brittleness when the failure strain data is not available.

### Damage distribution parameter $F_0$

The influence of the model parameters listed as the reference parameters previously on the damage distribution parameter  $F_0$  is analysed by changing one of the corresponding parameters and leaving the other parameters constant.

The effects of confining stress, joint cohesion and joint friction angle on the damage distribution parameter  $F_0$  is demonstrated in Fig. 9a, b, and c, respectively. The results show that the damage distribution parameter  $F_0$  follows the ‘U’ shape with various joint orientation, reaching the minimum value when joint orientation equals to  $45 + \phi_j/2$ .

The confining stress can increase the level of damage distribution parameter as confining stress increases from 0 to 20 MPa (see Fig. 9a). However, it has a larger influence on  $F_0$  when joint orientation  $\beta = 0^\circ$  and  $\beta = 90^\circ$  but smaller influence when joint orientation  $0^\circ < \beta < 90^\circ$ . This is due to the fact that two failure modes occur: shear failure when joint orientation  $\beta = 0^\circ$  and  $\beta = 90^\circ$  and sliding failure when joint orientation  $0^\circ < \beta < 90^\circ$ .

The joint cohesion effect on  $F$  is investigated by increasing cohesion from 2 to 10 MPa (see Fig. 9b). The maximum value of  $F_0$  is independent with different joint cohesion as the maximum failure strength keeps unchanged with a certain confining condition. On the other hand, joint cohesion can increase the values of  $F_0$  when it is less than the maximum value of  $F_0$ . As joint cohesion increases, the  $F_0$  gradually reaches its maximum value when joint orientation approaching to horizontal and vertical directions.

The joint friction angle effect on  $F_0$  is analysed by varying from 0 to  $40^\circ$  (see Fig. 9c). Similarly, the joint friction angle has no influence on the maximum value of  $F_0$ . The interval of ‘U’ shape narrows from smaller joint orientation as joint



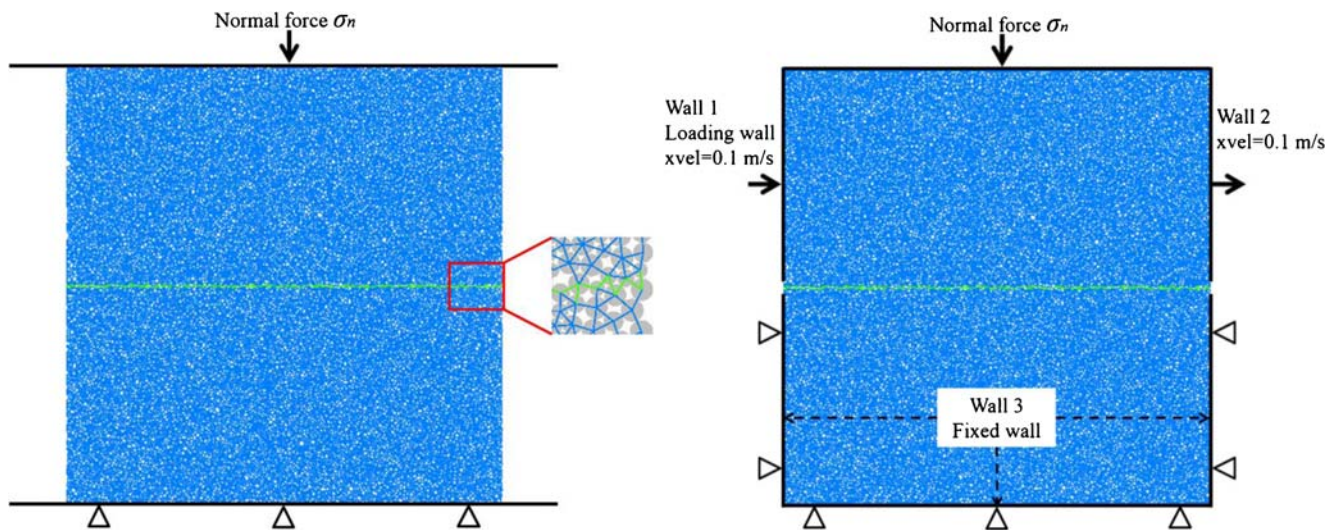


Fig. 6 Calibration of smooth-joint micro-parameters for PFC analysis. (a) Uniaxial compression test. (b) Direct shear test

friction angle increases. At the same time, the joint friction angle can increase the value of  $F_0$  when it is less than the maximum value. Overall, the  $F_0$  can be regarded as a strength parameter, indirectly related to the failure strength of the jointed rock masses.

### Influence of joint stiffness on the damage variable and rock mass response

Based on derived damage distribution parameters  $m$  and  $F_0$ , the rock mass response will be influenced by the joint orientation. However, as pointed out earlier in “[Damage model implementation](#)” section, the joint stiffness may have effects on the rock mass response, which was ignored by the previous studies (Liu and Yuan 2015; Zhang et al. 2015).

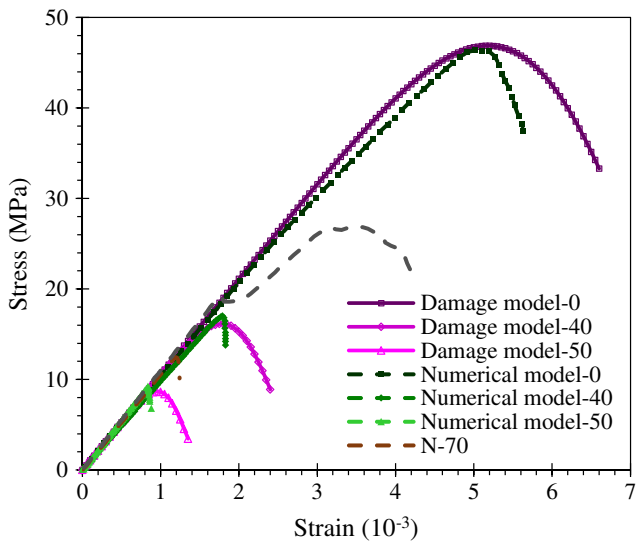
Invoking Eq. (23), the deformation modulus of the rock masses varies with joint orientation. When the  $\delta$  and stiffness ratio (normal stiffness/shear stiffness) are set to 1 m and 0.5, respectively, we plot the deformation modulus versus joint orientation as the normal stiffness increases from 10 to 200 GPa (see Fig. 10). The results show that the deformation modulus decreases as the joint orientation becomes smaller. The joint stiffness has a larger influence on the deformation modulus when the jointed rock mass with small joint orientation than those with larger joint orientation, even has no influence when the joint orientation equals to  $90^\circ$ .

To better investigate the joint stiffness effect, based on the theoretical analysis, using the parameters of the reference, the rock mass response, damage variable  $D$  and damage evolution rate  $D_r$  curves with and without considering the joint stiffness are plotted in Fig. 11. When the joint stiffness effect on the  $D$ ,  $D_r$  and rock mass response is ignored, the deformation modulus of the jointed rock mass equals to Young’s modulus of intact rock. The results reveal that all the damage variable  $D$ , damage evolution rate  $D_r$  and rock mass response curves of the model with  $0^\circ$ ,  $10^\circ$ ,  $20^\circ$ ,  $30^\circ$  and  $40^\circ$  overlap with those models with  $90^\circ$ ,  $80^\circ$ ,  $70^\circ$ ,  $60^\circ$  and  $50^\circ$ , respectively. The failure strength varies with varying joint orientation when deformation modulus is kept constant. The damage variable  $D$  curve becomes steeper, and the starting damage point appears earlier as joint orientation approaching  $40^\circ$  and  $50^\circ$ . Correspondingly, the maximum value of  $D_r$  becomes smaller as the joint orientation approaching  $40^\circ$  and  $50^\circ$ .

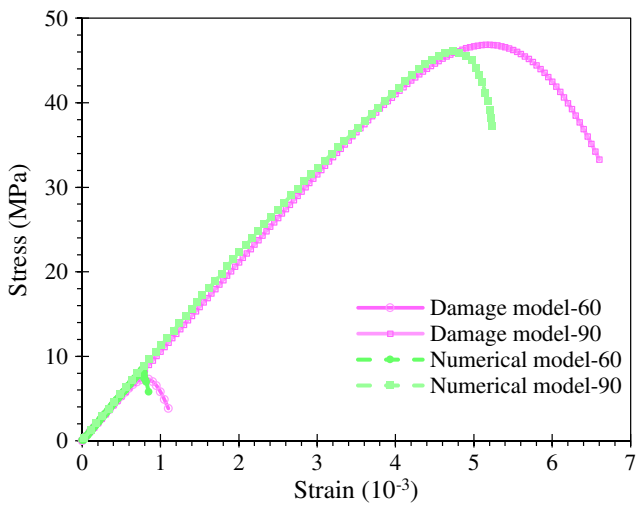
The joint normal stiffness is set to 50 GPa when considering the joint stiffness. One can easily see that the deformation modulus varies from the stress-strain curves, consisting of the experimental results given in “[Validation of the proposed damage model](#)” section. The results demonstrate that damage variable  $D$  curve becomes steeper, and the starting point of damage variable  $D$  appears earlier as the joint stiffness increases. Additionally, the peak value of damage evolution rate  $D_r$  becomes larger with

**Table 3** Calibrated micro-parameters for the smooth-joint model

Calibrated micro-parameters	Normal stiffness (GPa/m)	Shear stiffness (GPa/m)	Friction angle ( $^\circ$ )	Cohesion (MPa)	Tensile strength (MPa)
Value	800	200	32	2.20	1



**a** Joint orientation 0°, 40° and 50°.



**b** Joint orientation 60° and 90°.

**Fig. 7** Comparison of the proposed damage model and PFC model predictions for the jointed rock mass with various joint orientation. **a** Joint orientation 0°, 40° and 50°. **b** Joint orientation 60° and 90°

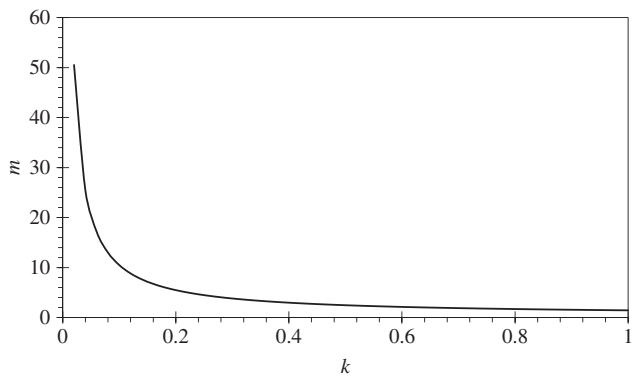
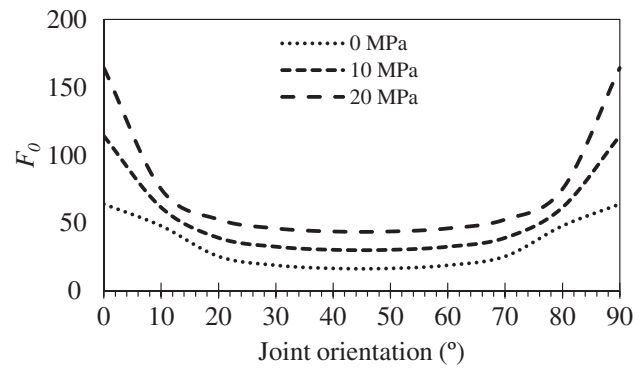
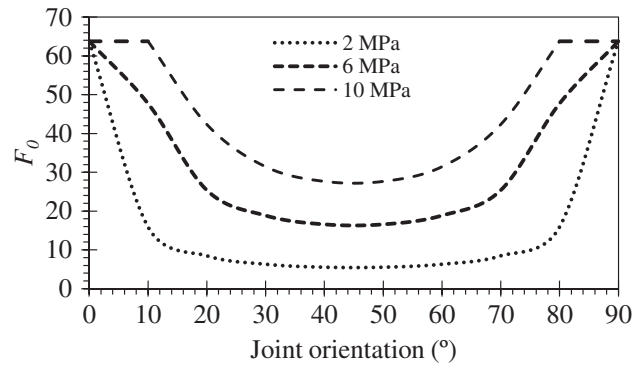


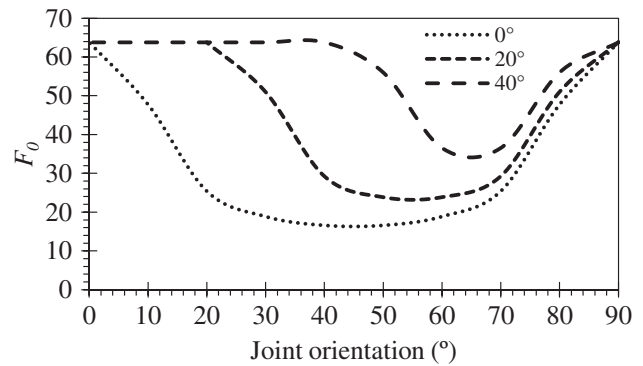
**Fig. 8** Damage distribution parameter  $m$  versus parameter  $k$



**a** Confining stress



**b** Joint cohesion



**c** Joint friction angle

**Fig. 9** Influence of **a** confining stress, **b** cohesion and **c** joint friction angle on the damage distribution parameter  $F_0$

increasing joint stiffness. Therefore, the proposed damage model considering joint stiffness can better capture the deformation and strength behaviours compared with the damage model without considering joint stiffness.

### Conclusions

In this paper, we proposed a new damage model which uses the Jaeger's and modified Hoek-Brown criteria. The damage distribution parameters  $m$  and  $F_0$  were modified to reflect the

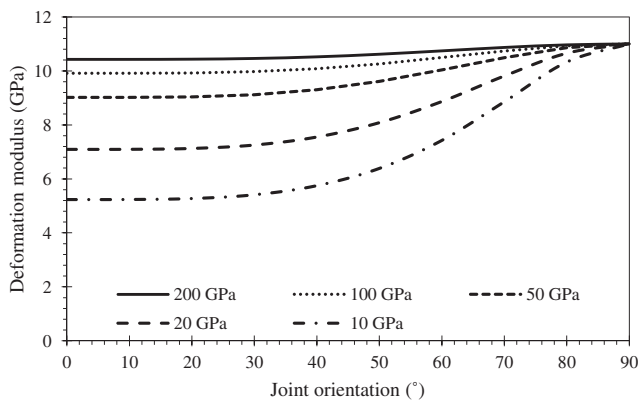


**Fig. 10** Influence of joint stiffness on the deformation modulus of the rock masses

effect of joint orientation on the rock mass failure behaviour. This way, we can simulate the jointed rock mass behaviours with various joint orientations realistically. Additionally, the

deformation modulus variation caused by the joint stiffness can be considered in the damage model by introducing the deformation modulus from Eq. (23). Based on this research, the following conclusions are obtained:

- (1) The shape parameter  $m$  was only related to the introduced strain parameter  $k$ , reflecting the brittleness of the anisotropic rock mass;
- (2) The damage variable  $D$  and rock mass response demonstrated an anisotropic characteristic for the damage model with various joint orientations. The damage variables and stress-strain curves for with the orientations of  $0^\circ$ ,  $10^\circ$ ,  $20^\circ$ ,  $30^\circ$  and  $40^\circ$  coincided with those of  $90^\circ$ ,  $80^\circ$ ,  $70^\circ$ ,  $60^\circ$  and  $50^\circ$ , respectively, when joint stiffness was ignored in the proposed damage model.
- (3) The proposed damage model can reflect the failure modes of the jointed rock mass if the Jaeger’s criterion was employed. Therefore, it improves the prediction of

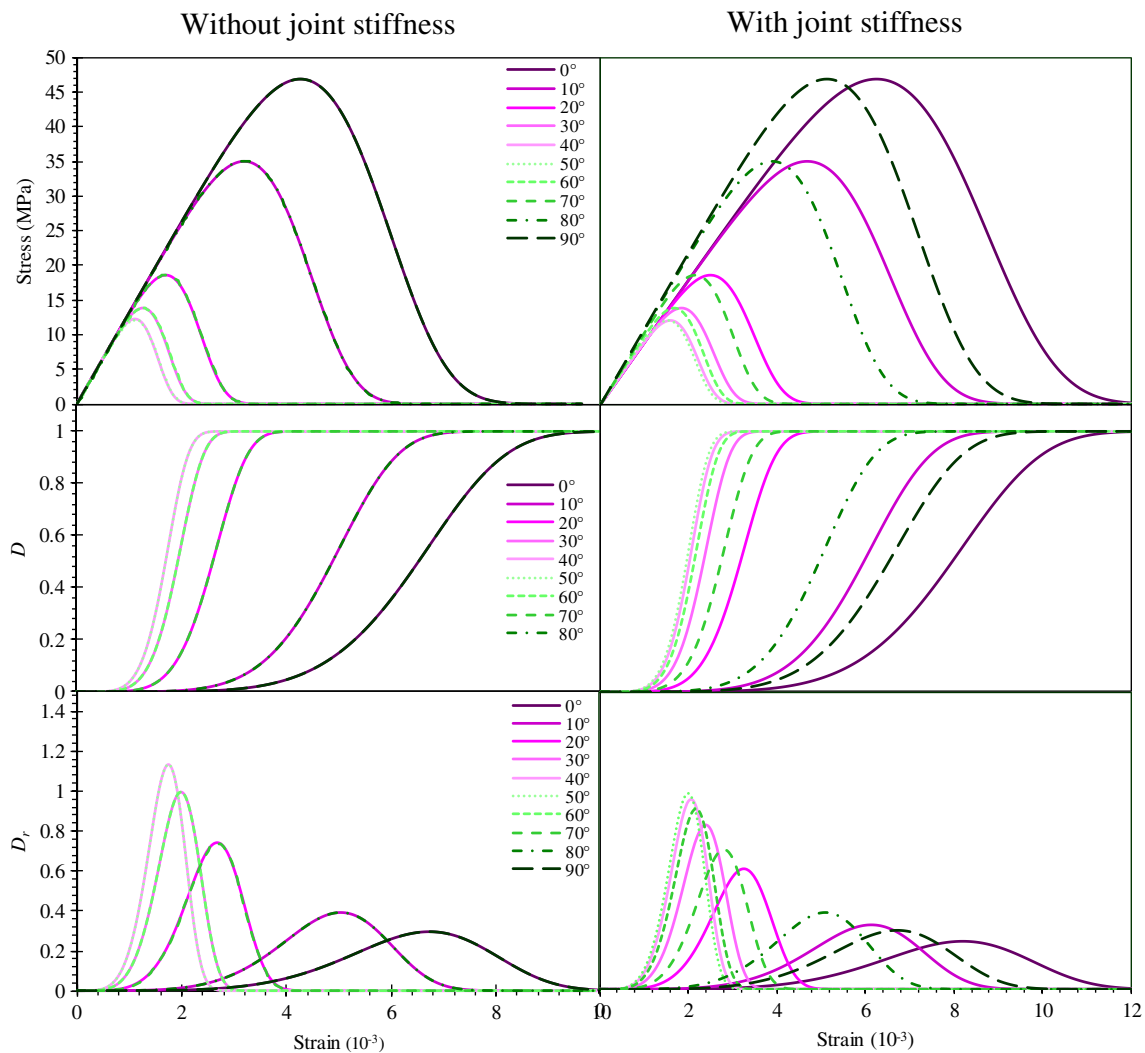


**Fig. 11** Influence of joint stiffness on rock mass response, damage variable  $D$  and damage evolution rate  $D_r$  for rock masses with different joint orientation

rock mass response significantly; thus, the proposed model can be used to simulate anisotropic rock mass behaviour accurately.

**Acknowledgments** The PhD scholarship provided by the China Scholarship Council (CSC) to the first author is gratefully acknowledged.

## References

- Bahaaddini M, Sharrock G, Hebblewhite BK (2013) Numerical direct shear tests to model the shear behaviour of rock joints. *Comput Geotech* 51:101–115
- Cao W, Zhao H, Li X, Zhang Y (2010) Statistical damage model with strain softening and hardening for rocks under the influence of voids and volume changes. *Can Geotech J* 47:857–871
- Cao W, Tan X, Zhang C, He M (2018) A constitutive model to simulate the full deformation and failure process for rocks considering initial compression and residual strength behaviors. *Can Geotech J* 13:1–13. <https://doi.org/10.1139/cgj-2018-0178>
- Chen YF, Wei K, Liu W, Hu SH, Hu R, Zhou CB (2016) Experimental characterization and micromechanical modelling of anisotropic slates. *Rock Mech Rock Eng* 49:3541–3557
- Deng J, Gu D (2011) On a statistical damage constitutive model for rock materials. *Comput Geosci* 37:122–128
- Donath F (1961) Experimental study of shear failure in anisotropic rocks. *Geol Soc Am Bull* 72:985–990
- Gao C, Xie LZ, Xie HP, He B, Jin WC, Sun YZ (2016) Estimation of the equivalent elastic modulus in shale formation: theoretical model and experiment. *J Pet Sci Eng* 151:468–479
- Guo S, Qi S, Zhan Z, Zheng B (2017) Plastic-strain-dependent strength model to simulate the cracking process of brittle rocks with an existing non-persistent joint. *Eng Geol* 231:114–125
- Hoek E (1964) Fracture of anisotropic rock. *J South Afr Inst Min Metall* 64:501–518
- Hudson JA, Harrison JP (2000) *Engineering rock mechanics: an introduction to the principles*. Elsevier, Amsterdam. <https://doi.org/10.1016/B978-008043010-2/50000-9>
- Jia P, Yang TH, Yu QL (2012) Mechanism of parallel fractures around deep underground excavations. *Theor Appl Fract Mech* 61:57–65
- Jiang Q, Feng XT, Hatzor YH, Hao XJ, Li SJ (2014) Mechanical anisotropy of columnar jointed basalts: an example from the Baihetan hydropower station, China. *Eng Geol* 175:35–45
- Jin C, Li S, Liu J (2016) Anisotropic mechanical behaviors of columnar jointed basalt under compression. *Bull Eng Geol Environ* 77:1–14
- Kawamoto T, Ichikawa Y, Kyoya A, (1988) Deformation and fracturing behaviour of discontinuous rock mass and damage mechanics theory. *Int. J Numer Anal Methods Geomech* 12:1–30
- Kostić S (2017) Analytical models for estimation of slope stability in homogeneous intact and jointed rock masses with a single joint. *Int J Geomech* 17:04017089
- Krajcinovic D, Silva MAG (1982) Statistical aspects of the continuous damage theory. *Int J Solids Struct* 18:551–562. [https://doi.org/10.1016/0020-7683\(82\)90039-7](https://doi.org/10.1016/0020-7683(82)90039-7)
- Li X, Cao W, Su Y (2012) A statistical damage constitutive model for softening behavior of rocks. *Eng Geol* 143–144:1–17
- Li X, Wang S, Weng L, Huang L, Zhou T, Zhou J (2015) Damage constitutive model of different age concretes under impact load. *J Cent South Univ* 22:693–700. <https://doi.org/10.1007/s11771-015-2572-0>
- Liu H, Yuan X (2015) A damage constitutive model for rock mass with persistent joints considering joint shear strength. *Can Geotech J* 52: 1136–1143
- Mas Ivars D, Potyondy D, Pierce M, Cundall P (2008) The smooth-joint contact model, in: *Proceedings of WCCM8-ECCOMAS*, 2008, 8th. Venice, Italy
- Mas Ivars D, Pierce ME, Darcel C, Reyes-Montes J, Potyondy DO, Paul Young R, Cundall P a (2011) The synthetic rock mass approach for jointed rock mass modelling. *Int J Rock Mech Min Sci* 48:219–244
- Mclamore R, Gray KE (1967) The mechanical behavior of anisotropic sedimentary rocks. *J Eng Ind* 89:62–73
- Peng J, Rong G, Cai M, Zhou CB (2015) A model for characterizing crack closure effect of rocks. *Eng Geol* 189:48–57
- Pierce M, Cundall P, Potyondy D, Mas Ivars D (2007) A synthetic rock mass model for jointed rock, in: *Meeting society's challenges and demands*, 1st Canada-US rock mechanics symposium, Vancouver pp 341–349
- Potyondy DO, Cundall PA (2004) A bonded-particle model for rock. *Int J Rock Mech Min Sci* 41:1329–1364
- Prudencio M, Van Sint Jan M (2007) Strength and failure modes of rock mass models with non-persistent joints. *Int J Rock Mech Min Sci* 44:890–902
- Ramamurthy T, Rao G, Singh J (1988) A strength criterion for anisotropic rocks. In: *Fifth Australia-New Zealand Conference on Geomechanics*. pp 253–257
- Saroglou H, Tsiambaos G (2008) A modified Hoek-Brown failure criterion for anisotropic intact rock. *Int J Rock Mech Min Sci* 45:223–234
- Shen J, Karakus M (2014) Simplified method for estimating the Hoek-Brown constant for intact rocks. *J Geotech Geoenviron Eng* 140: 04014025
- Swoboda G, Shen XP, Rosas L (1998) Damage model for jointed rock mass and its application to tunnelling. *Comput Geotech* 22:183–203.
- Tang CA, Kaiser PK (1998) Numerical simulation of cumulative damage and seismic energy release during brittle rock failure—part I: fundamentals. *Int J Rock Mech Min Sci*
- Tang CA, Yang WT, Fu YF, Xu XH (1998) A new approach to numerical method of modelling geological processes and rock engineering problems-continuum to discontinuum and linearity to nonlinearity. *Eng Geol* 49:207–214
- Tien YM, Tsao PF (2000) Preparation and mechanical properties of artificial transversely isotropic rock. *Int J Rock Mech Min Sci* 37:1001–1012
- Tiwari RP, Rao KS (2006) Post failure behaviour of a rock mass under the influence of triaxial and true triaxial confinement. *Eng Geol* 84:112–129
- Ulusay R (2014) *The ISRM suggested methods for rock characterization, testing and monitoring: 2007–2014*. Springer, Berlin
- Vallejos JA, Salinas JM, Delonca A, Mas Ivars D (2016) Calibration and verification of two bonded-particle models for simulation of intact rock behavior. *Int J Geomech* 17:06016030
- Wang ZL, Li YC, Wang JG (2007) A damage-softening statistical constitutive model considering rock residual strength. *Comput Geosci* 33:1–9. <https://doi.org/10.1016/j.cageo.2006.02.011>
- Wasantha PLP, Ranjith PG, Viete DR (2013) Specimen slenderness and the influence of joint orientation on the uniaxial compressive strength of singly jointed rock. *J Mater Civ Eng* 26:06014002
- Wasantha PLP, Ranjith PG, Zhang QB, Xu T (2015) Do joint geometrical properties influence the fracturing behaviour of jointed rock? An investigation through joint orientation. *Geomech Geophys Geo Energy Geo Resour* 1:3–14
- Xu XL, Karakus M (2018) A coupled thermo-mechanical damage model for granite. *Int J Rock Mech Min Sci* 103:195–204
- Yang ZY, Chen JM, Huang TH (1998) Effect of joint sets on the strength and deformation of rock mass models. *Int J Rock Mech Min Sci* 35: 75–84

- Yang SQ, Xu P, Ranjith PG (2015) Damage model of coal under creep and triaxial compression. *Int J Rock Mech Min Sci* 80:337–345. <https://doi.org/10.1016/j.ijrmms.2015.10.006>
- Yang W, Zhang Q, Ranjith PG, Yu R, Luo G, Huang C, Wang G (2019) A damage mechanical model applied to analysis of mechanical properties of jointed rock masses. *Tunn Undergr Space Technol* 84:113–128. <https://doi.org/10.1016/j.tust.2018.11.004>
- Zhang XP, Wong LNY (2013) Loading rate effects on cracking behavior of flaw-contained specimens under uniaxial compression. *Int J Fract* 180:93–110
- Zhang XP, Wong LNY (2014) Choosing a proper loading rate for bonded-particle model of intact rock. *Int J Fract* 189:163–179
- Zhang L, Hou S, Liu H (2015) A uniaxial compressive damage constitutive model for rock mass with persistent joints considering the joint shear strength. *Electron J Geotech Eng* 20:5927–5941
- Zhao G, Xie L, Meng X (2014) A damage-based constitutive model for rock under impacting load. *Int J Min Sci Technol* 24:505–511. <https://doi.org/10.1016/j.ijmst.2014.05.014>
- Zhao H, Zhang C, Cao WG, Zhao MH (2016) Statistical meso-damage model for quasi-brittle rocks to account for damage tolerance principle. *Environ Earth Sci* 75:862
- Zhou Y, Wu SC, Gao YT, Misra A (2014) Macro and meso analysis of jointed rock mass triaxial compression test by using equivalent rock mass (ERM) technique. *J Cent South Univ* 21:1125–1135d
- Zhou S, Xia C, Zhao H, Mei S, Zhou Y (2017) Statistical damage constitutive model for rocks subjected to cyclic stress and cyclic temperature. *Acta Geophys* 65:893–906
- Zhou C, Xu C, Karakus M, Shen J (2018) A systematic approach to the calibration of micro-parameters for the flat-jointed bonded particle model. *Geomech Eng* 16:471–482. <https://doi.org/10.12989/gae.2018.16.5.471>
- Zhou C, Xu C, Karakus M, Shen J (2019) A particle mechanics approach for the dynamic strength model of the jointed rock mass considering the joint orientation. *Int J Numer Anal Methods Geomech*:2797–2815. <https://doi.org/10.1002/nag.3002>